Spin Injection into a Superconductor with Strong Spin-Orbit Coupling

T. Wakamura,[1] N. Hasegawa,[1] K. Ohnishi,[1] Y. Niimi,[1] and YoshiChika Otani[1,2,*]
[1]Institute for Solid State Physics, University of Tokyo, Kashiwa-no-ha 5-1-5, Kashiwa, Chiba 277-8581, Japan
[2]RIKEN-CEMS, 2-1 Hirosawa, Wako, Saitama 351-0198, Japan
(Received 8 October 2013; published 24 January 2014)

We demonstrate spin injection into superconducting Nb by employing a spin absorption technique in lateral spin valve structures. Spin currents flowing in a nonmagnetic Cu channel are preferably absorbed into Nb due to its strong spin-orbit interaction, the amount of which dramatically changes below or above the superconducting critical temperature (T_C). The charge imbalance effect observed in the Cu/Nb interface ensures that superconducting Nb absorbs pure spin currents even below T_C. Our analyses based on the density of states calculated using the Usadel equation can well reproduce the experimental results, implying that the strong spin-orbit interaction of Nb is still effective for the spin absorption even below T_C. Most importantly, our method allows us to determine the intrinsic spin relaxation time in the superconducting Nb, which reaches more than 4 times greater than that in the normal state.

DOI: 10.1103/PhysRevLett.112.036602 PACS numbers: 72.25.Ba, 72.25.Mk, 74.45.+c, 74.78.Na

The recent development of nanofabrication technology has led to the contemporary evolution of the novel discipline of spintronics, which is beneficial for both condensed matter physics and applied nanoscience [1]. Superconductivity might also be the discipline that could evolve in combination with spintronics since it exhibits a vast variety of interesting phenomena at the same length scale, such as the proximity effect and the Andreev reflection [2]. Combining superconductors with spintronics thus brings about novel phenomena such as the spin charge separation in superconducting Al in high magnetic fields [3,4] and peculiar transport properties like the moderate spin relaxation, as predicted by the theoretical study [5].

As to the spin transport, the spin relaxation time (τ_{sf}) of superconductors is sometimes controversial experimentally: 10^6-fold enhancement of τ_{sf} of superconducting Al confined in a magnetic double tunnel junction has been experimentally shown [6], while other studies reported that the τ_{sf} is shorter than [7] or equivalent to [8] that in the normal state. One should note that in previous studies, spurious effects like the magnetic proximity effect on a superconductor [7] or the charging effect in a small tunnel junction [8] render unambiguous interpretation difficult. It is therefore essential to inject a pure spin current into superconductors out of the proximity to ferromagnets to avoid such ambiguity.

In this Letter we report on the spin injection into superconducting Nb. Our device structure enables us to determine τ_{sf} of superconducting Nb free from the superfluous effects mentioned above. Compared with previous studies, Nb is employed as a superconductor because it is more intriguing in that it can bring about novel phenomena like the spin Hall effect due to its strong spin-orbit (SO) interaction, and it has even higher superconducting critical temperature (T_C) than Al. We used the spin absorption technique, which is efficient for injecting a pure spin current into materials with strong SO interaction [9,10]. Below T_C, the amount of the absorbed spin current anomalously depends on the spin injection current. Calculations based on the Usadel equation can well reproduce the experimental results and show that the spin current is absorbed into superconducting Nb considering the superconducting gap of Nb with the proximity effect and the strong SO interaction. Our calculations can directly estimate τ_{sf} in the superconducting state and demonstrate that it becomes more than 4 times longer than that in the normal state, consistent with the theoretical prediction [5].

Two types of samples were prepared for the spin absorption experiments by means of electron-beam lithography and the shadow evaporation technique. One is the typical lateral spin valve structure [11,12] (sample A), where two ferromagnetic ($Ni_{81}Fe_{19}$, hereafter Py) wires are bridged by a nonmagnetic (Cu) wire. The other sample (sample B) has the same structure as sample A, except that a Nb wire is inserted below Cu in between the two Py wires [9,10], as depicted in Fig. 1. We prepared a methyl-methacrylate

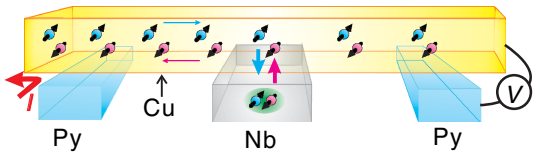

FIG. 1 (color online). Schematic image of the spin absorption experiment. The Nb middle wire is inserted between two Py wires in the lateral spin valve structure. We flow the spin injection current I between Cu and one of two Py wires to generate a pure spin current in Cu. The pure spin current is partially absorbed into the Nb middle wire. The signal is detected as a voltage V between Cu and the other Py.

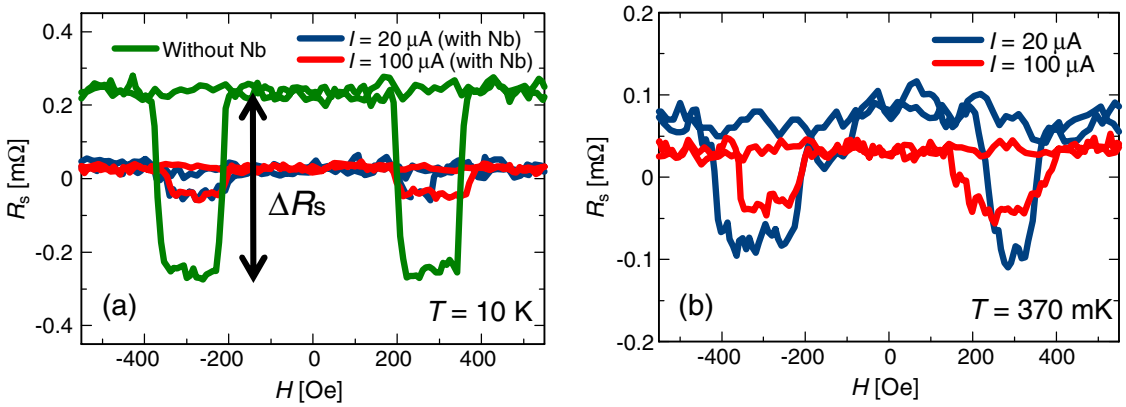

FIG. 2 (color online). The NLSV signal above T_C [(a), $T = 10$ K] and below T_C [(b), $T = 370$ mK]. The green (gray) curve is obtained from the sample without the Nb middle wire (sample A), and the red (dark gray) and the blue (black) curves are from the sample with Nb (sample B). The red and the blue curves are different in I. For $T > T_C$, they show almost the same value, much less than the green curve. However, for $T < T_C$, they become different and the blue one shows an almost 2 times larger value than the red one. Double curves for each color are from the different sweeps.

and polymethyl-methacrylate double layer resist onto a thermally oxidized silicon substrate. After the lithography, a 20 nm thick Py film was deposited on the substrate using an electron-beam evaporator with a certain angle, and then a 20 nm thick Nb from the counter direction keeping the deposition rate for the homogeneous T_C. The thickness of Nb was chosen so as to keep the sufficient T_C and not to disturb the spin transport in the Cu bridge. Then a 100 nm thick Cu was deposited normal to the substrate with a thermal evaporator. The targets of Nb and Cu are both spatially separated from the Py target, in order to make Nb and Cu free from magnetic impurities. These procedures were carried out without breaking the vacuum. The pressure was kept below 10^{-9} Torr during the deposition. The widths of Py, Nb, and Cu wires are 100, 300, and 100 nm, respectively. The Nb middle wire becomes superconducting below 5.5 K ($\equiv T_C$).

The transport measurements were performed in a ^{3}He cryostat by using a standard lock-in technique with an ac excitation current of 173 Hz. We flowed a spin injection current I from one of the two Py wires (injector) to Cu to generate the spin accumulation in Cu. The generated pure spin current in the Cu bridge is detected as a voltage V between the other Py (detector) and Cu [see Fig. 1]. During the measurement an external in-plane magnetic field H is applied parallel to the longitudinal axis of the Py wires, and V shows different values according to their parallel or antiparallel magnetization [11,12]. The nonlocal spin valve (NLSV) signal ΔR_s is defined as a difference in the measured nonlocal voltage divided by I; i.e., $R_s = V/I$. If an extra wire (middle wire) with large SO interaction (here Nb) is inserted between the two Py wires, the spin current in Cu is partly absorbed into Nb for the benefit of its fast spin relaxation [9,10]. As a result, the amount of the spin current that reaches the detector is reduced, and thus the spin absorption can be detected as the decreasing NLSV signal.

We first measured R_s for both samples at 10 K, above T_C. ΔR_s is suppressed in sample B compared with that in sample A [Fig. 2(a)]. This explicitly shows that the spin current is absorbed into the Nb middle wire because of its strong SO interaction. From the ratio $\Delta R_s^{\text{with}}/\Delta R_s^{\text{without}}$, we calculated the spin relaxation length (λ_{sf}) of Nb (see Supplemental Material [13]) and obtained $\lambda_{\text{sf}} = 6$ nm. We note that ΔR_s is independent of I, as shown in blue ($I = 20$ μA) and red ($I = 100$ μA) curves in Fig. 2(a). These results are consistent with our previous studies [10,12].

We next cooled the sample down to 370 mK, much lower than T_C and measured R_s again. Surprisingly, ΔR_s obtained with $I = 20$ μA was much larger than that with $I = 100$ μA [Fig. 2(b)]. In order to clarify the relation between ΔR_s and I in more detail, we measured ΔR_s, with increasing I. As shown in Fig. 3, while ΔR_s at $T = 10$ K ($> T_C$) is almost independent of I (triangles), ΔR_s at 370 mK ($< T_C$) increases with I below 100 μA (circles). At $I = 10$ μA, it is dramatically enhanced to more than 2 times the value for $I = 100$ μA.

For elucidating the effect of the superconductivity of Nb on this anomalous I dependence of ΔR_s, we investigated the interface state at the Cu/Nb junction since the interface is the most influential to the spin absorption. We flowed an ac current i through the Nb/Cu junction and detected the voltage v between Nb and Cu, as shown in the inset of Fig. 4(a). The interface resistance R_I is defined as $R_I \equiv v/i$. Figure 4(a) shows the T dependence of R_I. R_I was measured with the excitation current i of 1 μA, much smaller than I. Above T_C, R_I shows a negative value. This can be explained by the inhomogeneous current flow at the interface, as pointed out in many previous studies on the giant magnetoresistance effect [14,15], and has nothing to do with superconductivity. With decreasing T, we observed a sharp peak at T_C, and the sign of R_I changed from negative to positive below T_C. This peak at T_C and

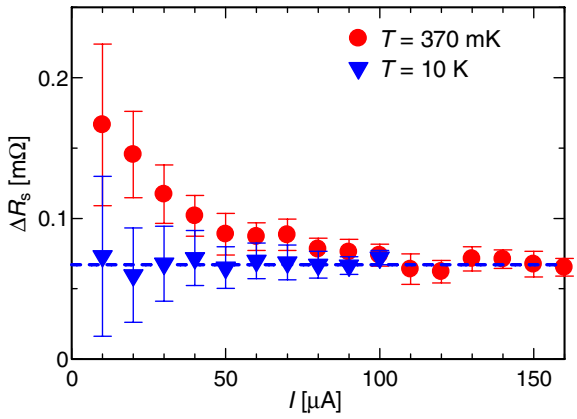

FIG. 3 (color online). The relation between the NLSV signal ΔR_s and the spin injection current I. When $T = 10$ K (above T_C), ΔR_s is almost independent of I (triangles). However, when $T = 370$ mK (below T_C), ΔR_s increases as I decreases (circles).

extra resistance below T_C arise from the charge imbalance effect, related to the charge relaxation process of quasiparticles in superconductors as reported first in the 1970s [16]. The properties of the charge imbalance effect are also discussed recently, especially for the low temperature properties [17], the spatial evolution [18,19] and the spin polarized electrons [20]. The result of the charge imbalance effect in Fig. 4(a) assures us that for $T < T_C$, the area close to the Cu/Nb interface is in the superconducting state.

We then fixed T at 370 mK and plotted R_I as a function of the spin injection current I in Fig. 4(b). R_I was measured with an ac current i as in Fig. 4(a), while flowing a dc spin injection current I. The obtained curve appears very similar to the R_I as a function of T [Fig. 4(a)]. The similarity of these two curves indicates that the spin injection current I is proportional to the effective temperature $T_{\rm eff}$ at the Cu/Nb interface [13]. The overall tendency in Fig. 4(b) is still sustained with applied in-plane magnetic field. Therefore, by comparing Figs. 4(a) and 4(b), we can conclude that when the sign of R_I is positive, the interface is superconducting, which is satisfied in the NLSV measurement for $I < 150$ μA (corresponding to T_C) with an in-plane magnetic field.

In order to investigate the effect of the superconducting gap of Nb on the spin absorption, we calculated the density of states (DOS) in the superconducting Nb. Since the interface between Nb and Cu is transparent, we have to consider the proximity effect between them [2]. The DOS of Nb in proximity to Cu can be obtained by solving the one-dimensional Usadel equation [21,22]:

$$\frac{\hbar D}{2}\frac{\partial^2\theta}{\partial x^2} + \left(iE - \frac{\hbar}{2\tau_{\rm sf}}\cos\theta\right)\sin\theta + \Delta(x)\cos\theta = 0. \quad (1)$$

In this equation, D is the diffusion constant and x is the coordinate with $x = 0$ at the interface. θ is a complex function of x and E and describes the pair correlation. $\Delta(x)$ is the superconducting pair potential and can be calculated as follows:

$$\Delta(x) = N_S(0)\mathcal{V}\int_0^{\hbar\omega_D} \tanh\left(\frac{E}{2k_BT}\right)\mathrm{Im}[\sin\theta]dE, \quad (2)$$

where $N_S(0)$, $\mathcal{V}$, and ω_D are the DOS of Nb in the normal state, the pairing interaction strength, and the Debye frequency, respectively. We solved Eq. (1) in combination with Eq. (2). The DOS of the superconducting Nb normalized by $N_S(0)$ is expressed as $n_S(E) = \mathrm{Re}[\cos\theta]$. In the inset of Fig. 5, we show an example of $n_S(E)$ in the vicinity of the Nb/Cu interface (orange triangles) and far from the interface (blue squares). The DOS of Nb near the interface has an energy gap but is smeared out due to the proximity effect and the large spin relaxation in Nb. The ratio of the spin current (I_s) flowing through the Nb/Cu interface between superconducting and normal state is expressed as [5,23]

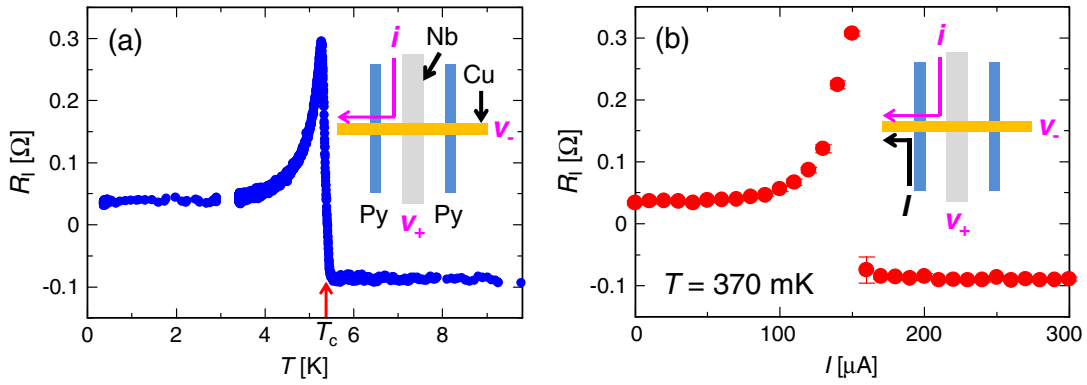

FIG. 4 (color online). (a) Temperature dependence of R_I. The sharp peak at $T = T_C$ and extra resistance below T_C originate from the charge imbalance effect and are related to the superconductivity of Nb. (b) Dependence of R_I on the spin injection current I. The same curve is obtained as (a). The insets show the measurement setup for R_I.

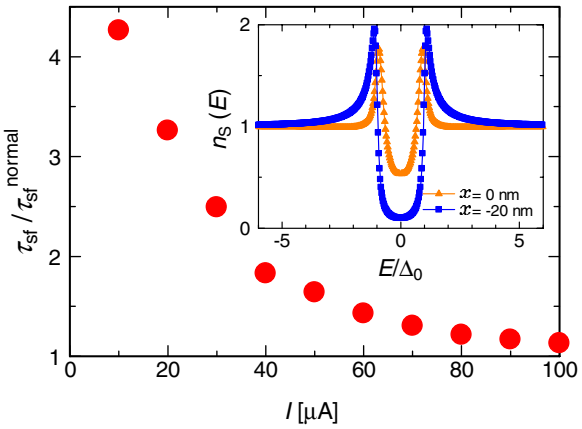

FIG. 5 (color online). The relation between τ_{sf} and I. τ_{sf} is normalized by that in the normal state ($\tau_{sf}^{normal} = 2.3 \times 10^{-13}$ s). As I decreases, τ_{sf} dramatically increases. Inset: DOS of superconducting Nb calculated by the Usadel equation for $x = 0$ nm and $x = -20$ nm.

$$\frac{I_s^{super}}{I_s^{normal}} = \int_{-\infty}^{\infty} n_S(E)\left(-\frac{\partial f_0(E)}{\partial E}\right)dE. \quad (3)$$

The details of the calculation are in [13]. This equation demonstrates that the spin current absorption explicitly reflects the normalized DOS of superconducting Nb, $n_S(E)$. The relation between the ratio of ΔR_s and I_s in the superconducting or normal state is written as [13]

$$\frac{\Delta R_s^{super}}{\Delta R_s^{normal}} = \frac{Q_{Nb}^{super} I_s^{super}}{Q_{Nb}^{normal} I_s^{normal}}, \quad (4)$$

where $Q_{Nb}^{super(normal)} = \mathcal{R}_{Nb}^{super(normal)}/\mathcal{R}_{Cu}$, $\mathcal{R}_{Nb}^{super(normal)}$ is the spin resistance of the Nb middle wire in the superconducting (normal) state and $\mathcal{R}_{Cu}$ is the spin resistance of Cu [24]. We note that the change of $\mathcal{R}_{Cu}$ due to the proximity effect is negligible because it is found from the calculation that the proximity effect in Cu is small and spatially limited while $\mathcal{R}_{Cu}$ is defined in the whole Cu wire. From the experimentally measured ΔR_s, we can determine Q_{Nb} [9,13]. Thus, we can obtain I_s^{super}/I_s^{normal} from the experimental values. For reproducing the experimental values of I_s^{super}/I_s^{normal}, we calculate Eq. (3) treating τ_{sf} as a free parameter in Eq. (1). By this technique we can directly obtain τ_{sf}, without calculating the quantities such as the resistivity of quasiparticles usually necessary for calculating τ_{sf}. Changing τ_{sf}, we can reproduce ΔR_s^{super}, and we acquired appropriate τ_{sf} for each I. The obtained τ_{sf} normalized by that in the normal state (τ_{sf}^{normal}) is shown in Fig. 5. As I decreases, τ_{sf} dramatically increases. When $I = 10$ μA, τ_{sf} is more than 4 times larger than that of the saturated value for $I > 100$ μA. The saturated value of $\tau_{sf} \sim 2.5 \times 10^{-13}$ s for $I > 100$ μA is fairly close to τ_{sf} in the normal state of Nb: $\tau_{sf}^{normal} \sim 2.3 \times 10^{-13}$ s, calculated from the relation $\tau_{sf} = \lambda_{sf}^2/D$. This correspondence supports the validity of our analysis. Considering the relation between I and T_{eff}, increasing τ_{sf} with decreasing I is consistent with increasing τ_{sf} with decreasing T_{eff}, as predicted in the theory [5].

Now we discuss the relation between the anomalous I dependence of ΔR_s and the superconductivity of Nb. When I is large ($I \sim 100$ μA, for example), the DOS is relatively suppressed due to the gap opening near $E \sim 0$, but it is not so effective on the spin transport because $-\partial f_0(E)/\partial E$ is broadened due to the relatively large effective temperature near the Cu/Nb interface in Eq. (3). When I is decreasing, the gap largely opens, and the DOS at $E \sim 0$ is highly suppressed. Since $-\partial f_0(E)/\partial E$ is nonzero only at $E \sim 0$, the spin injection is suppressed by the reduced DOS in this energy range.

Finally, we mention the increased spin relaxation time. In our sample structure, we can avoid superfluous effects such as the magnetic proximity effect [7] or the charging effect [8] which made the accurate estimation of τ_{sf} difficult in previous studies. According to the theory, the spin relaxation time τ_{sf} is related to the impurity scattering time τ_{imp}, which is related to the DOS as $\tau_{imp} \propto N(E)^{-1}$ [25], where $N(E)$ is the DOS. The reduced DOS enhances the spin relaxation time τ_{sf} due to the gap opening; hence, $N(E) = 0$ in the gap [5]. In our study, the increment is more than 4 times, but still less than the previous study [6]. This is mainly due to the smeared superconducting gap in our case, while it is even sharper in Ref. [6] where Al was confined in magnetic double tunnel junctions.

In conclusion, we have studied the spin injection into the superconducting Nb. A pure spin current is absorbed into Nb even in its superconducting state, and the anomalous NLSV signal dependence on the spin injection current is well explained by the calculation based on the Usadel equation. Our calculations allow us to directly estimate the spin relaxation time of superconducting Nb in the structure without spurious effects and demonstrate that it is enhanced by more than 4 times that in the normal state, consistent with the theoretical prediction.

The authors acknowledge helpful discussions with T. Kato and M. Okada. We would also like to thank Y. Iye and S. Katsumoto for the use of the lithography facilities. This work was supported by KAKENHI.

*yotani@issp.u-tokyo.ac.jp

[1] I. Žutić, J. Fabian, and S. Das Sarma, Rev. Mod. Phys. **76**, 323 (2004).
[2] S. Guéron, H. Pothier, N. O. Birge, D. Esteve, and M. H. Devoret, Phys. Rev. Lett. **77**, 3025 (1996).
[3] F. Hübler, M. J. Wolf, D. Beckmann, and H. von Löhneysen, Phys. Rev. Lett. **109**, 207001 (2012).
[4] C. H. L. Quay, D. Chevallier, C. Bena, and M. Aprili, Nat. Phys. **9**, 84 (2013).

[5] T. Yamashita, S. Takahashi, H. Imamura, and S. Maekawa, Phys. Rev. B **65**, 172509 (2002).
[6] H. Yang, S.-H. Yang, S. Takahashi, S. Maekawa, and S. S. P. Parkin, Nat. Mater. **9**, 586 (2010).
[7] Y.-S. Shin, H.-J. Lee, and H.-W. Lee, Phys. Rev. B **71**, 144513 (2005).
[8] C. D. Chen, W. Kuo, D. S. Chung, J. H. Shyu, and C. S. Wu, Phys. Rev. Lett. **88**, 047004 (2002).
[9] Y. Niimi, Y. Kawanishi, D. H. Wei, C. Deranlot, H. X. Yang, M. Chshiev, T. Valet, A. Fert, and Y. Otani, Phys. Rev. Lett. **109**, 156602 (2012).
[10] M. Morota, Y. Niimi, K. Ohnishi, D. H. Wei, T. Tanaka, H. Kontani, T. Kimura, and Y. Otani, Phys. Rev. B **83**, 174405 (2011).
[11] F. J. Jedema, A. T. Filip, and B. J. van Wees, Nature (London) **416**, 713 (2002).
[12] T. Wakamura, K. Ohnishi, Y. Niimi, and Y. Otani, Appl. Phys. Express **4**, 063002 (2011).
[13] See Supplemental Material at http://link.aps.org/supplemental/10.1103/PhysRevLett.112.036602 for the relation between the spin injection current and the effective temperature, and the derivation of the equations appearing in the main text.
[14] J. M. Pomeroy and H. J. Grube, J. Appl. Phys. **105**, 094503 (2009).
[15] J. S. Moodera, L. R. Kinder, J. Nowak, P. LeClair, and R. Meservey, Appl. Phys. Lett. **69**, 708 (1996).
[16] J. Clarke, Phys. Rev. Lett. **28**, 1363 (1972).
[17] F. Hübler, J. Camirand Lemyre, D. Beckmann, and H. v. Löhneysen, Phys. Rev. B **81**, 184524 (2010).
[18] R. Yagi, K. Tsuboi, R. Morimoto, T. Matsumura, and H. Kobara, J. Phys. Soc. Jpn. **78**, 054704 (2009).
[19] K. Yu. Arutyunov, H.-P. Auraneva, and A. S. Vasenko, Phys. Rev. B **83**, 104509 (2011).
[20] P. Cadden-Zimansky and V. Chandrasekhar, Phys. Rev. Lett. **97**, 237003 (2006).
[21] K. D. Usadel, Phys. Rev. Lett. **25**, 507 (1970).
[22] W. Belzig, F. K. Wilhelm, C. Bruder, G. Schön, and A. D. Zaikin, Superlattices Microstruct. **25**, 1251 (1999).
[23] T. Yamashita, H. Imamura, S. Takahashi, and S. Maekawa, Phys. Rev. B **67**, 094515 (2003).
[24] S. Takahashi and S. Maekawa, Phys. Rev. B **67**, 052409 (2003).
[25] S. Takahashi, T. Yamashita, H. Imamura, and S. Maekawa, J. Magn. Magn. Mater. **240**, 100 (2002).